Use of LDH- chromate adsorption co-product as an air purification photocatalyst

A. Nehdi[1], N. Frini-Srasra[1,2], G. de Miguel[3], I. Pavlovic[4,*], L. Sánchez[4] and J.Fragoso[4,*]

[1]Laboratoire des Matériaux Composites et Minéraux Argileux, Centre National de Recherche en Sciences des Matériaux CNRSM, Technopôle Borj Cedria, BP 73, 8027 Soliman, Tunisie

[2]Faculty of Sciences of Tunis (FST), Manar University, Tunisia.

[3]Departamento de Química Física y Termodinámica Aplicada, Instituto Universitario de Nanoquímica IUNAN, Universidad de Córdoba, Campus de Rabanales, E-14014 Córdoba, España.

[4]Departamento de Química Inorgánica, Instituto Universitario de Nanoquímica IUNAN, Universidad de Córdoba, Campus de Rabanales, E-14071 Córdoba, Spain.

* Corresponding Authors:

- Ivana Pavlovic

  ORCID ID: 0000-0003-2165-2940

  E-mail: iq2pauli@uco.es

  Tel: +00-34-957-218648

- Javier Fragoso

  ORCID ID: 0000-0002-1041-6574

  E-mail: q32frnuj@uco.es

  Tel: +00-34-957-218634

Abstract

This work deals with the use of layered double hydroxides for a double environmental remediation. The residue obtained in the use of these materials as a chromate sorbent in water, was subsequently studied as a photocatalyst for the removal of NOx gases. With this aim, MgAl-CO_3 layered double hydroxides were synthesized by the coprecipitation method with a divalent/trivalent metal ratio of 3. After its calcination at 450 °C, the mixed oxide was obtained and MgAl-CrO_4 were synthesized by the reconstruction method. A complete chemical, morphological and photochemical study of the samples was carried out with techniques such as XRD, FT-IR, TGA, XRF, PL, DRIFTS and UV-Vis spectroscopy. Results showed that LDH materials presented no significant changes in their structure after their use as a sorbent. Photocatalytic tests of the samples showed a very good NO removal efficiency, as well as a high selectivity (low NO_2 emissions) through complete oxidation of these oxides to nitrate. The incorporation of chromate into the LDH structure improved the absorption of light in the visible region of the spectra, producing an improvement of 20 % in the NO elimination compared with the LDH without chromate.

Keywords: LDH, Hydrotalcite, Chromate, Photocatalyst, Nitrogen Oxides

1. Introduction

Layered double hydroxides (LDH), also known as hydrotalcite like materials, are an important class of lamellar anionic clays, which have been attracting scientific attention in recent decades. Due to their unique properties and easy and inexpensive synthesis, these materials have been widely studied for many applications in different fields such as catalysis (Olszówka et al., 2018; Zhou et al., 2017), pharmacy (Acharya et al., 2019; Kim et al., 2020), polymer stabilizers (Taviot-Guého et al., 2018), flame control (Jin et al., 2020), electrochemistry (González et al., 2016) photocatalysis (Mantilla et al., 2010; Parida et al., 2012) etc. They have a brucite-like structure where divalent metal ions are partially substituted by trivalent ones, and a positive charge thus generated is balanced by the arrangement of hydrated anions in the interlayer (Cavani et al., 1991; Rives, 2001). The composition of LDH may be expressed by the general formula $[M^{II}_{1-x}M^{III}_{x}(OH)_2]^{x+}[A^{n-}]_{x/n}\cdot mH_2O$ where M^{II} = Mg, Zn, Ni, etc. M^{III} = Al, Cr, etc., A= CO_3^{2-}, NO_3^-, Cl^- etc., *x* is the value that determines the layer charge density and the anion exchange capacity, and ranges between 0.2 – 0.4. One of the peculiarities of these compounds is when calcined at 500 °C, they are converted into mixed oxides, which recover the LDH structure in the presence of anions in aqueous solutions ("memory effect").

These versatile materials can be considered as doped semiconductors where the doping agent is the transition metal cation located at the octahedral sites of the brucite sheets. The high LDH photocatalytic activity is due to the easy mobility and separation of electrons and holes created in these materials (Parida and Mohapatra, 2012), as well as to the surface OH^- groups which can react with holes in the valence band and produce hydroxyl radicals, a key intermediary in photo-oxidative reactions (Lv et al., 2020).

We recently reported excellent LDH photocatalytic activity for the degradation of NO_x gases (DeNOx process) (Huo et al., 2019a; Rodriguez-Rivas et al., 2018). These gases (NO_x = NO + NO_2), emitted from industrial and traffic sources, are classified as priority air pollutants in urban zones (European Environment Agency, 2019). They participate in the formation of tropospheric ozone which, when inhaled, produce respiratory problems, reduce lung function and in general, many early deaths are associated with NO_x emissions (Chen et al., 2004). Titania is the standard photocatalyst used for DeNOx applications, but it is only active under UV light ($\lambda < 387$ nm; 3.2 eV energy band gap) and not under visible light irradiation. Moreover, TiO_2 exhibits a low DeNOx selectivity. If we consider NO $\rightarrow$ NO_2^- $\rightarrow$ NO_2 $\rightarrow$ NO_3^- as the basic photocatalytic mechanism, a huge emission of NO_2, a gas much more toxic than NO, occurs during the process. However, LDH materials, besides high photocatalytic activity, also showed an outstanding selectivity (no NO_2 emissions) for the DeNOx process. Thus, LDH could be a highly efficient alternative to TiO_2 in the battle for NOx abatement.

On the other hand, one of the widely studied LDH applications is as adsorbents for water pollutants. Due to the exchangeability of interlayer anions and, the so called memory effect of its calcined product, LDH have attracted great interest for removing many inorganic and organic anions from contaminated waters (Chaara et al., 2012; Otero et al., 2013; Paikaray et al., 2013; Pavlovic et al., 2013). The chromate ion is a very harmful water pollutant due to its mutagenicity, genotoxicity, bioaccumulation and carcinogenicity. It can reach surface and groundwaters as an effluent of different industries such as chrome plating, fertilizers, batteries, leather, textile, etc (Fei and Liu, 2016; Kaprara et al., 2015; Koleli and Demir, 2016), as well as from filtration from metal mines or inadequate handling of mining supplies (Ukhurebor et al., 2021). One of the proposed methods for chromate removal from waters is through its adsorption on LDH and its

calcined product, and there are many reports claiming its high adsorption capacity for this pollutant (Chao et al., 2018; del Arco et al., 2006; Hsu et al., 2019; Lazaridis et al., 2004; Lu et al., 2016; Prasanna et al., 2006; Tran et al., 2019). Howeverthe desorption of adsorbed contaminants and the regeneration of adsorbents is the most difficult and expensive part of an adsorption technology, which could elevate the total cost for an adsorption system up to 70 % (Goh et al., 2008).

The purpose of this study is to assess the reuse of the MgAl-CrO_4 adsorption residue as a desirable good in the field of photocatalysis. Thus, this work deals a double environmental remediation technology: removal of pollutants from water (chromate ion) and from air (NOx gases) by using a single starting component, calcined MgAl-LDH. In a first step, the MgAl LDH is used to remove chromate ions from water. Secondly, once the MgAl-CrO_4 was collected and dried, this co-product was reused for the photocatalytic NOx removal from air. For this last process, an enhanced response is expected due to the presence of interlayer chromate ions, in similarity to that found for the chemistry parent compound molybdate which electronic structure assists to the formation of electron/hole pairs (Mohapatra et al., 2012). The structural, morphological and optical properties of LDH chromate adsorbate are fully characterized. The changes observed are commented on with relation to their ability to perform photocatalytic DeNOx processes. The chromate containing sample shows a high photochemical activity, the oxidation mechanism being explained in the light of the results obtained by using EPR, PL and DRIFT techniques.

2. Methods and materials

2.1 Synthesis of the photocatalyst

The preparation of $Mg_3Al\text{-}CrO_4$ proceeded in two steps: firstly, a $Mg_3Al\text{-}CO_3$ LDH ("MgAl" sample) was prepared by the co-precipitation method at a constant pH = 10, at room temperature (Comelli et al., 2013). Then, 0.75 mol of $Mg(NO_3)_2.6H_2O$ and 0.25 mol of $Al(NO_3)_3.9H_2O$ mixed solution (250 mL) were added dropwise to 500 mL of magnetically stirred solution containing 1.7 mol of NaOH and 0.5 mol of Na_2CO_3. The suspension thus obtained was aged for 24 h at room temperature. Then, it was centrifuged and washed several times with distilled water to eliminate the presence of nitrates, and dried. The resulting product was then thermally treated in a furnace at 500 °C for 6 hours. 2 g of thus obtained Mg-Al mixed oxide (named MgAl/500) was added to a 100 mL of 0.05 M K_2CrO_4 solution and stirred during 24 h. to obtain reconstructed $Mg_3Al\text{-}CrO_4$ LDH (named MgAl-Cr). Then, it was centrifuged, washed several times and dried for 24 h at 90 °C.

2.2 Characterization of the samples

X-ray diffraction powder (XRD) patterns were obtained using a Bruker D8 Discover instrument, with Cu Kα radiation (λ = 1.5406 Å). Infrared spectra (IR) analyses were carried out on transmission mode in a FT-MIR Perkin Elmer FRONTIER with a resolution of 4 cm^{-1}. Chemical analyses were determined by X-ray fluorescence (XRF) on an ZSX Primus IV Rigaku. The water content of LDH was calculated from the thermogravimetric (TG) analysis which was obtained by using a Mettler Toledo apparatus in air atmosphere (flow: 100 mL min^{-1}) at a heating rate of 5 °C min^{-1}. Nitrogen adsorption–desorption isotherms were recorded in an ASAP 2020 apparatus (Micromeritics). Prior to the sorption measurements, samples were degassed at 100 °C under vacuum for 4 h. The morphological characterizations were done by scanning electron

136 microscopy (SEM) using a Jeol JSM 7800F microscope. Diffuse reflectance UV-Vis (DRS) spectra
137 of the samples were recorded from 200 to 800 nm employing a Cary 5000 spectrophotometer
138 with PTFE as reference.

139

140 *2.3. Photocatalytic activity evaluation*

141 Photocatalytic activity was examined analyzing the removal ratio of NO in a continuous-flow
142 reactor illuminated by a sunlight irradiation box (Solarbox 3000e RH; Xe lamp with irradiances of
143 25 and 580 $W \cdot m^{-2}$ for UV and visible light respectively). The reactor contained the LDH
144 photocatalyst. 300 mg of sample powder, supported in a 5x5 cm sample holder, was used in
145 each experiment. 500 ppb NO simulated polluted atmosphere flowed through the reactor (0.3 L
146 min^{-1}) with a relative humidity 50 ± 10 %. Firstly, the adsorption-desorption equilibrium between
147 gas and sample was assured for 10 min. Subsequently, the lamp was switched on for 30 min. The
148 concentration of NO was continuously measured by a NO_X chemiluminescence analyzer
149 (Environnement-AC32M).

150 Electron paramagnetic resonance (EPR) technique assisted in corroborating the radical
151 species involved in the photocatalytic process. The spectra were recorded at room temperature
152 in a Bruker-EMX micro spectrometer. The spin-trap 5,5-Dimethyl-1-pyrroline N-oxide (DMPO,
153 Sigma-Aldrich) was used for radical detection. Water or methanol solutions were prepared for
154 detecting ·OH or $\cdot O_2^-$ radicals, respectively. The photocatalyst specimen was immersed in a 45
155 mM DMPO solution and irradiated for 30 min with sunlight. Photoluminescence (PL)
156 measurements were carried out in a FLS920 Fluorimeter (Edinburgh Instrument Ltd, Livingston,
157 UK). A 450 W Xe lamp was employed as the excitation source in the steady-state measurements
158 and a picosecond pulsed diode laser (l_{exc} = 406 nm and pulse width = 87 ps) was used for the

159 time-resolved measurements. In order to find out about the photochemical DeNOx mechanism,
160 in situ diffuse reflectance infrared Fourier transform spectroscopy (DRIFTS) measurements were
161 performed using a Perkin Elmer FRONTIER FT-IR spectrometer equipped with a Harrick reaction
162 chamber. The sample was placed in the reaction chamber, treated at room temperature under
163 high-purity Ar flow for 10 minutes to remove environmental impurities. Subsequently, in the
164 dark, a mixture of 50 mL/min NO (100 ppm) and 50 mL/min O_2 was pumped into the chamber,
165 the sample being subjected to adsorption reactions for 25 minutes. Afterwards, light was turned
166 on for 60 min. The spectra evolving in both periods were sequentially recorded every 5 minutes.

167

168 ## 3. Results and discussion

169 *3.1 Characterization of photocatalysts*

170 The MgAl and MgAl-Cr XRD patterns (**Figure 1a**) were both identified as hydrotalcite-like
171 compounds indexed in a rhombohedral lattice (Cavani et al., 1991). MgAl-Cr shows strong (00l)
172 plane reflections, which confirms the rehydration and reconstruction of the mixed oxide
173 MgAl/500 (**Figure S1**) into the LDH, after its exposure to an aqueous solution of chromate anions.
174 The first two peaks at 10-11°/2θ and 22-23°/2θ correspond to the basal reflections 00l, which in
175 the case of MgAl-Cr are shifted to the right indicating a decrease in its interlayer space,
176 compared to those of MgAl from d = 7,87 Å to d= 7,72 Å (**Figure 1a**). The shortening of the
177 interlayer distance in these layered structures is related to the grafting of CrO_4^{2-} to the metal
178 hydroxide slab by displacing OH^- molecules (del Arco et al., 2004). After grafting, the interlayer
179 anions are better attached to the layers and are much more difficult to exchange with other
180 anions (Costantino et al., 1997). This is very important for the scavenging of toxics as it will
181 prevent the eventual leaching of chromate ions from the hydrotalcite interlayer. On the other

182 hand, a part of the chromate anions could be adsorbed by a surface complexation at the edges
183 of hydrotalcite particles (Jobbágy and Regazzoni, 2013). The patterns were indexed in a
184 rhombohedral lattice with a values [a =$2d_{(110)}$] 3.06 Å and c values 23.13 Å and 23.438 Å
185 [c=$3d_{(003)}$] corresponding to MgAl and MgAl-Cr, respectively. The crystal size was D=90.4nm for
186 MgAl and 90.2nm for MgAl-Cr.

187 The Fourier Transform Infrared (FT-IR) spectra of both samples are shown in **Figure 1b**, being
188 characteristic of LDH compounds. In both cases, a broad band observed around 3500 cm^{-1}
189 corresponds to the stretching vibrations of the hydrogen-bonded hydroxyl group of both
190 hydroxide layers and interlayer water molecules, while the band at ~1639 cm^{-1} is attributed to O-
191 H bending vibration of water molecules. The MgAl sample exhibits a strong band at 1360 cm^{-1},
192 which corresponds to the asymmetric stretching mode of carbonate interlayer anions. However,
193 the presence of a weaker carbonate band (1366 cm^{-1}) is also observed in MgAl-Cr because,
194 despite the precautions taken during the synthesis, some intercalation of carbonate is difficult to
195 avoid, due to its high reactivity and affinity for the hydrotalcite interlayer. Chromate
196 incorporation in the LDH structure is verified by the appearance of an absorption band at 863
197 cm^{-1}, which corresponds to the stretching frequency ν (Cr–O) (del Arco et al., 2006). Compared
198 to the free anion, this band is slightly shifted toward lower frequencies (27 cm^{-1}), indicating the
199 lowering of symmetry of the chromate ion in the LDH interlayer (Malherbe et al., 1999; Prasanna
200 et al., 2006). Absorptions below 800 cm^{-1} are due to lattice vibrations, involving metal–oxygen
201 stretching modes.

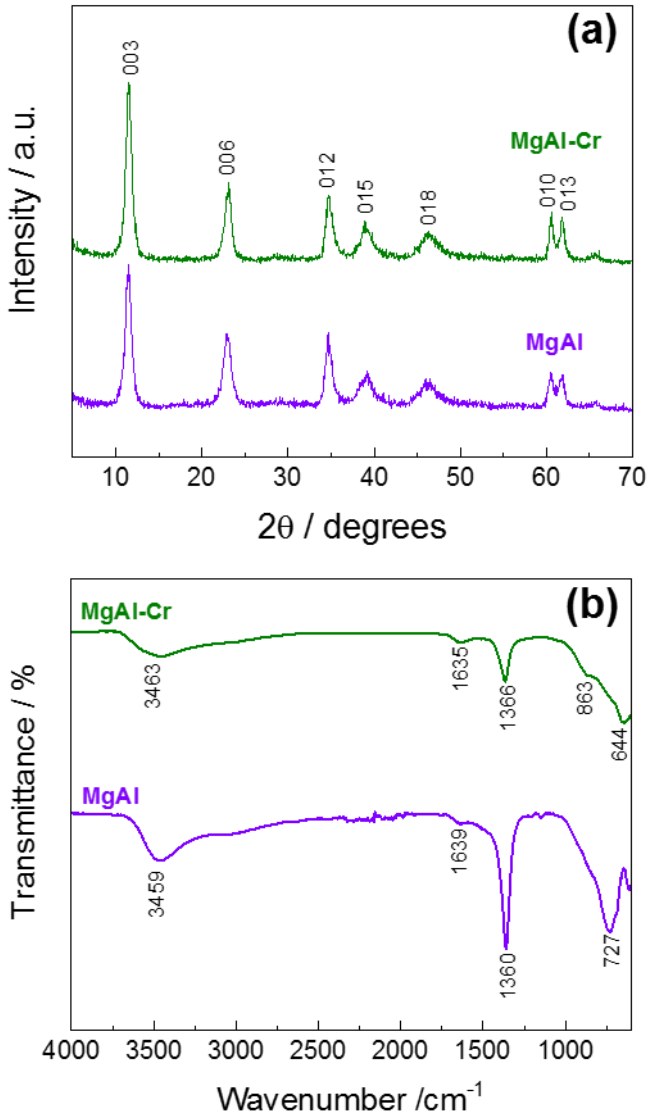

202

Figure 1. *(a) XRD patterns and (b) IR spectra obtained from the MgAl and MgAl-Cr samples.*

203 The chemical analysis of the original and modified MgAl-LDH is shown in **Table 1**. In both
204 cases, the Mg:Al molar ratio is similar to that of the starting solution. **Figure S2** shows that the
205 thermal behavior of Mg–Al LDH is characterized by two main steps: up to 250 °C the physisorbed
206 and interlayer water is lost, while at 250–500 °C the simultaneous dehydroxylation and
207 decarbonization processes take place and the LDH converts into a MgAl mixed-oxide (Frost et al.,
208 2005; Rives, 2001) (**Figure S1**). The amount of interlayer water, determined by the
209 thermogravimetric curves from the first weight loss, together with the Mg/Al molar ratio

obtained by XRF analysis were used to propose the chemical formula of the samples. It is inferred from these results that, based on this synthetic procedure, around 17 % of anions per LDH formula can be retained as chromate.

Table 1. *Physicochemical characterization for the LDH samples.*

	% w/w			M^{2+}/M^{3+} ratio	Proposed formula	S_{BET} (m^2g^{-1})	Lattice parameters		
LDH	Mg	Al	Cr				D (nm)	a (Å)	c (Å)
MgAl	23.5	8.68	<LOD	3	$[Mg_{0.75}Al_{0.25}(OH)_2](CO_3)_{0.125}\cdot 0.62H_2O$	30	92.4	3.06	23.13
MgAl-Cr	22.3	8.54	1.85	2.9	$[Mg_{0.745}Al_{0.255}(OH)_2](CrO_4)_{0.036}(CO_3)_{0.092}\cdot 0.69H_2O$	74	90.2	3.06	23.43

The morphology of the samples was evaluated by SEM observations, **Figure 2**. The MgAl sample appears as agglomerates of poor crystallized pseudo-hexagonal nanoparticles (**Figure 2a**). The reconstruction of the LDH structure during the inclusion of the chromate anion leads to a better crystallization and growth of the hexagonal particles, but also to the appearance of a high presence of smaller unshaped particles (**Figure 2b**). In consequence, the pore microstructure analyzed for the samples was somewhat different. **Figure S3** shows the N_2 adsorption-desorption isotherms measured for each sample. Slight differences were found on the isotherms shape. The presence of a hysteresis loop suggests the presence of mesopores, which were more pronounced in the case of the MgAl sample (from 2 to 40 nm; inset Figure S3a), fitting to a type IV isotherm. However, a large fraction of macropores was also observed in the case of the MgAl-Cr sample (from 50 to 160 nm; inset Figure S3b) exhibiting a type II shape (Rodriguez-Rivas et al., 2018), that assigned to the adsorption on macro and non-porous materials. The specific surface area values (SSA; BET method) for both samples are given in **Table 1**. As usually accounts for reconstructed LDHs an increase on SSA is observed (Rives, 2001). Thus, a significant value of 74 $m^2\cdot g^{-1}$ was measured for the MgAl-Cr sample, being more than double of

229 that exhibited by the MgAl sample, this being of importance for its potential use in
230 heterogeneous photocatalytic processes.
231

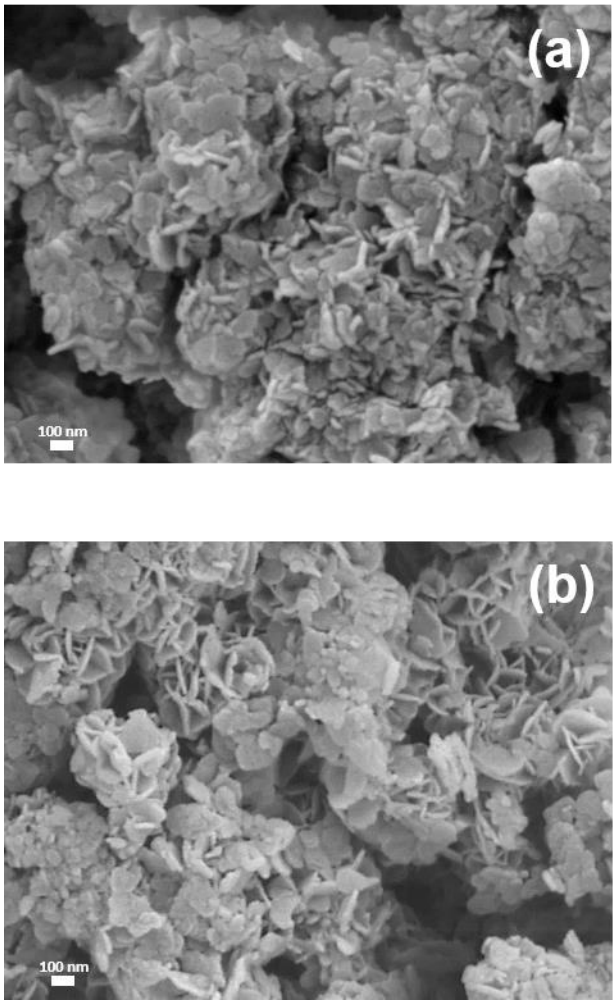

232

Figure 2. *SEM images of the (a) MgAl and (b) MgAl-Cr samples.*

233

234 Finally, in that concerning the characterization of the samples, the light absorption spectra
235 were recorded, Figure 3. The spectra obtained for the MgAl sample is similar to that previously
236 reported for this system (Gao et al., 2019). Because of its large band-gap value, Eg > 5.0 eV (Lv et
237 al., 2020; Mantilla et al., 2011), an intense peak at 220 nm is observed in the UV light region.
238 Considering the activation of environmental photocatalytic processes by sunlight, the

observation of bands at λ > 250 nm is most interesting. Thus, on this sample, a small absorption band at 305 nm in the UV light region, is observed, with a tail extending to the visible region until 430 nm. On the other hand, two intense UV bands are observed at 275 and 370 nm for the chromate intercalated sample, the last showing a shoulder in the visible light region at 445 nm. This spectra resembles that of chromate (VI) ions in solution and differs from those of samples containing insoluble chromate (VI) (Kuncewicz et al., 2011; Zheng et al., 2018), which could indicate the presence of CrO_4^{2-} ions grafted to metal hydroxide sheets. In summary, the spectra have shown that the chromate containing LDH sample exhibits a higher ability to harvest sunlight radiation.

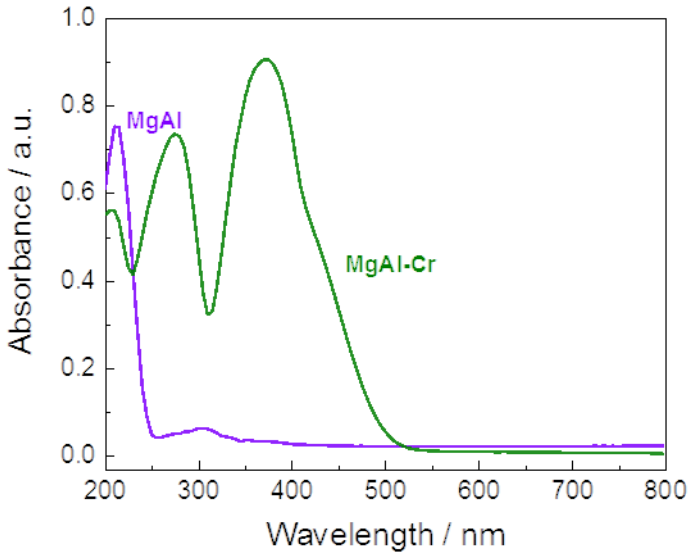

Figure 3. *UV-Vis absorption spectra of the MgAl and MgAl-Cr samples.*

3.2 Photocatalytic behaviour in DeNOx processes.

Once the chromate ion is retained in the LDH structure and the resulting LDH-chromate complex shows a noticeable light absorption ability, it is interesting to test its potential use in environmental remediation processes assisted by photocatalysis. Thus, the efficiency in the photocatalytic NO gas removal from air was studied as an air purification technique. This process

consists in promoting the photochemical oxidation (PCO) of nitrogen oxide gases to nitrite/nitrate (NO_2^-/NO_3^-) species, which are removed from air and retained on the surface of the photocatalyst. The successful use of different LDH as DeNOx photocatalysts has recently been reported (Fragoso et al., 2021; Pastor et al., 2020; Rodriguez-Rivas et al., 2020, 2018). Moreover, the MgAl-LDH system has also shown a modest activity in this process (Lv et al., 2020).

When the LDH photocatalyst is light irradiated, the electron in the valence band (VB) can acquire the necessary energy to jump to the conduction band (CB). Then, pairs of mobile charges (e^- and h^+) are generated and, once they reach the surface of photocatalyst particles, react with the adsorbed water and oxygen molecules. In consequence, reactive oxygen species (ROS), mainly hydroxide (·OH) and superoxide radicals ($\cdot O_2^-$) are formed, initiating a fast oxidation of nitrogen oxide gases because of their powerful oxidant character. The evolution of the nitrogen oxide concentration profiles in the presence of the MgAl-LDH samples were recorded with the function of light irradiation time, **Figure 4**. During the first ten minutes, because there was no light irradiation, the NO concentration in the reaction chamber remained constant to the inlet value. However, a sudden decrease in the NO concentration values occurred once the lamp was switched on, evidencing the participation of a light activated process (**Figures 4a and 4b**). For both samples, the PCO process reached a stationary state after fifteen minutes of light irradiation. Following these experiments, the ability of each sample to remove NO gas from air could be related with the decrease in NO concentration values under light irradiation. The modest NO removal efficiency of 40 % for the MgAl sample agrees with its low ability to harvest sunlight ($\lambda > 250$ nm), **Figure 4c**. However, a remarkable efficiency of 60 % was measured for the chromate containing sample; a value in line with the best reported for LDH DeNOx photocatalysts (Fragoso et al., 2021; Pastor et al., 2020; Rodriguez-Rivas et al., 2020). This test

proves that LDH chromate-sorbents can successfully be reused as air purification photocatalysts. Moreover, no emission of NO_2 gas was displayed during the PCO process (**Figures 4a and 4b**). NO_2 is an expected intermediate in this PCO process (Balbuena et al., 2015; Rodriguez-Rivas et al., 2020), but it must be avoided since it is much more toxic than NO (Lewis, 2012). Therefore, the MgAl-Cr sample is a highly efficient DeNOx photocatalyst, but also environmentally sustainable because there is no release of NO_2 gas. Finally, this photocatalyst was studied in successive DeNOx runs exhibiting a small loss of NO removal efficiency, **Figure 4d**.

The higher photocatalytic efficiency exhibited by MgAl-Cr, in comparison with MgAl, should be associated to their different microstructural and electronic properties. The higher specific surface area exhibited, once the LDH is reconstructed with CrO_4^{2-}, allows many active sites on particle surface to be available for the gaseous reactant molecules, increasing the process efficiency. On the other hand, the harvesting of the sunlight is remarkably done through the incorporation of chromate ions, which should eventually lead to a higher formation of ROS species and better photochemical activity. It is known that the electronic structure of a LDH could be influenced by different factors: the ionic nature and ratio of metal elements, as well as the nature of the interlayer anion (Wu et al., 2018). On the other hand, the important role of interlayer anions in the photocatalytic activity of LDHs has also been reported (Mohapatra and Parida, 2016). Therefore, changes in the electronic structure of MgAl-LDH are expected after the incorporation of CrO_4^{2-} ions. Because of its similarity to the molecular electronic structure, the participation of chromate on the LDH electronic structure should be considered like that reported for molybdate intercalated LDH (Mohapatra et al., 2012). Following the predicted molecular orbital energy level diagrams for tetrahedral oxyanions of transition elements, the non-bonding HOMO orbital of chromate is a fully filled oxygen 2p orbital, while the LUMO is the molecular orbital contributing Cr (3d orbital). Thus, ligand to metal charge transfer from HOMO

to LUMO should take place under light irradiation forming additional e^- and h^+ pairs, which favour a major production of ROS species.

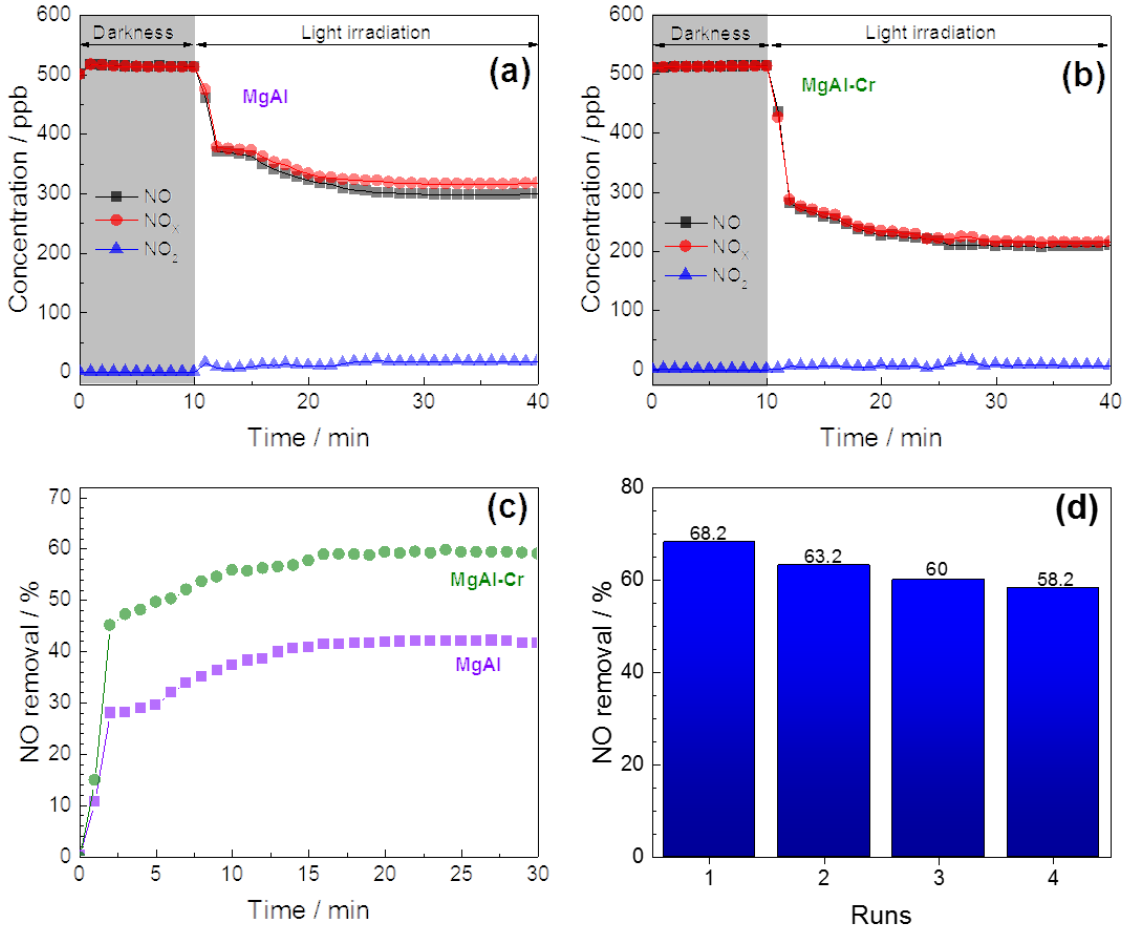

Figure 4. *NO, NO_2 and NO_x gases concentration evolution during the photo-degradation of gaseous NO under UV-Vis light irradiation on the (a) MgAl and (b) MgAl-Cr samples. (c) NO removal efficiency for both LDH samples. (d) No removal efficiency calculated for each run of the reusability tests for the MgAl-Cr sample.*

The EPR experiments are in line with the assumed electronic structure. Figure 5 shows the EPR signal obtained using MgAl-LDH as photocatalysts and DMPO as the spin-trapping agent under sunlight excitation, in aqueous and methanol solutions (**Figures 5a** and **5b**, respectively). No signal was obtained for the photocatalyst suspension (blank) in darkness. An identical signal for the DMPO-·OH adduct was registered for both examples, indicating a similar ability to

produce electron holes. However, in the case of the DMPO-·O_2^- signal huge differences were found, this signal being negligible for MgAl samples but very intense for MgAl-Cr. Therefore, the production of excited electrons seems to be favored by the presence of chromate ions, probably assisted by the injection of additional electrons from the HOMO → LUMO transition. In line with the results obtained from DeNOx tests, the clear production of superoxide radicals with the MgAl-Cr photocatalyst turns in a key factor enhancing the photochemical oxidation of NO gas.

An efficient charge separation and transfer of the photogenerated electron-holes is essential for the enhanced photocatalytic activity. To reveal the effect of chromate in the separation of electron-hole pairs, PL spectroscopy is employed to clarify the ability of the recombination of photogenerated species. **Figure S4** exhibits a PL band centred around 405 nm in the MgAl sample (λ_{exc} = 315 nm) while a red-shifted PL peak is detected around 560 nm for the MgAl-Cr sample (λ_{exc} = 400 nm). The MgAl-Cr sample was also excited at 315 nm but no PL was detected which indicates a different deactivation mechanism in both materials. The shift in the PL position is clear evidence of the presence of the chromate species in the MgAl-Cr sample. Thus, the addition of the chromate species modifies the energetics of the electronic bands opening a radiative mechanism at lower energy. In addition, **Figure 5** displays the PL decay of both samples where mono- or bi-exponential functions were used to fit the experimental data. Time constant of 0.67 and 3.05 ns were obtained for the MgAl sample (**Figure 5c**) in agreement with previous reports, while a longer time constant of 1341 ns was obtained for the MgAl-Cr sample (**Figure 5d**). The extended time for the excited electron-hole pairs in the MgAl-Cr sample forecasts a larger reaction with O_2 to generate the superoxide species, $\cdot O_2^-$, as previously observed in the EPR measurements.

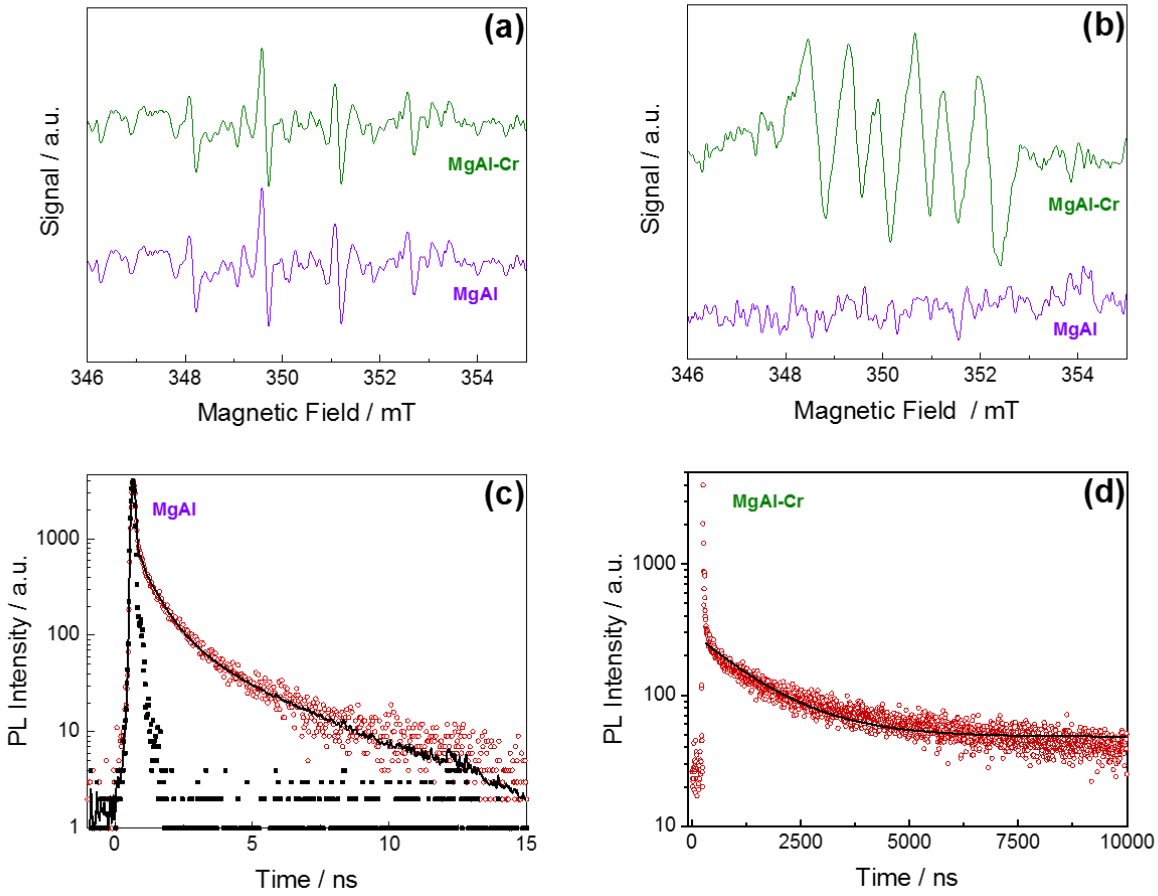

333

Figure 5. *DMPO spin-trapping EPR spectra of the MgAl and MgAl-Cr samples under UV-Vis light irradiation for 15 min in (a) aqueous solution for ·OH and (b) methanol solution for $\cdot O_2^-$. Decay times of the (c) MgAl and (d) MgAl-Cr samples.*

334

335 Finally, with the aim of discerning the photocatalytic removal mechanism of NO taking place
336 on the sample surface, in situ DRIFTS measurements were performed. Firstly, the NO adsorption
337 processes in the absence of light irradiation were analyzed. **Figure 6**, shows sequential spectra
338 obtained in dark conditions under NO flow for the MgAl-Cr sample, once the background
339 (spectrum obtained before NO flow) had been subtracted. During the first 5 minutes, signals
340 corresponding to nitrogen oxide species were registered. The appearance of NO^- (1126 cm^{-1}) and
341 NO_2^- species (830, 1355, 1424 and 1490 cm^{-1}) (Huo et al., 2019b; Li et al., 2019; Liao et al., 2020;
342 Zhang et al., 2018) is a consequence of the NO disproportionation in the presence of the

hydroxyl LDH groups (Liao et al., 2020); therefore the adsorption of NO occurs on this photocatalyst. These species were ultimately oxidized to nitrates (933, 961, 998 and 1019 cm^{-1})(Zhang et al., 2018). After 25 minutes, as higher amounts of NO came into contact with the surface, they also suffered oxidation to N_2O_4, signal at 908 cm^{-1} (Chen et al., 2020). Subsequently, the sample was light irradiated and then a sequential disappearance of lower oxidation nitrogen oxides species was observed, being photochemically oxidized to nitrate (961, 998 and 1019 cm^{-1}). The latter was the most abundant specie on the surface, the monodentate nitrate being gradually transformed with time into more stable bridged linkage (1227 cm^{-1}) (Chen et al., 2020). Moreover, during the irradiation period signals of NO_2 or N_2O_4 were not observed, in line with the high DeNOx selectivity shown by this photocatalyst.

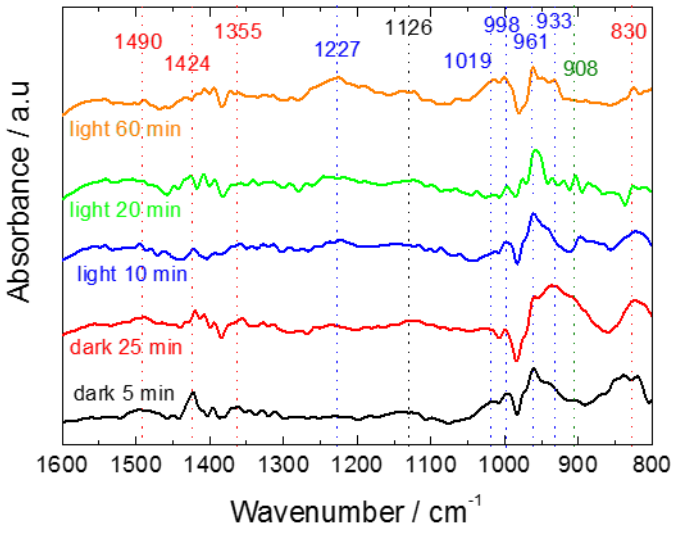

Figure 6. *DRIFTS spectra of MgAl-Cr, NO adsorption un darkness and NO oxidation processes under light illumination.*

4. Conclusions

Mixed oxide obtained by calcination of MgAl LDH is proved as an efficient sorbent to capture chromate ions from aqueous solutions. Compared to the pristine MgAl-CO_3 LDH, the

reconstructed LDH containing chromate exhibits a modified morphology, different micropore structure and higher specific surface. Moreover, the presence of CrO_4^{2-} anions enhances the ability of the LDH sample to absorb UV and Visible light. These characteristics promote the use of MgAl-Cr as a promising photocatalyst. In fact, good efficiency for NO removal is measured, which is oxidized towards nitrate on the photocatalyst surface under light irradiation. Interestingly, MgAl-Cr performs as an ecofriendly photocatalyst as no emissions of toxic NO_2 are accounted for during the PCO process. EPR and PL results highlight the role of chromate in the enhanced photoactivity, facilitating the production of photoexcited electrons and retarding the electron-hole recombination. The obtained results point out that LDH co-products obtained from water depollution tasks are valuable for additional environmental processes, the air purification through photocatalysis in this case, opening an interesting field of study in environmental chemical engineering.

Credit author statement

A.Nehdi: Investigation N.Frini-Srasra: Funding acquisition, Supervision G. de Miguel: Investigation, Writing and Reviewing. Pavlovic: Conceptualization, Writing, Review and Editing; Visualization L. Sánchez: Conceptualization, Writing, Review and Editing, Proyect administration J. Fragoso: Investigation, Validation, Writing, Review and Editing, Visualization

Acknowledgments

This collaboration was carried out with Borj Cedria research center “CNRSM” (LMCMA laboratory research group), Tunisian government. Amina Nehdi appreciate the efforts of Tunisian Ministry of Scientific Research. This work was partly financed by Junta de Andalucía (PAI Groups FQM-214

and FQM-175) and Spanish Government (MAT2017-88284-P). Javier Fragoso acknowledges the grant from Ministerio de Ciencia, Innovación y Universidades (PRE2018-084594 grant).

References

Acharya, R., Alsharabasy, A.M., Saha, S., Rahaman, S.H., Bhattacharjee, A., Halder, S., Chakraborty, M., Chakraborty, J., 2019. Intercalation of shRNA-plasmid in Mg-Al layered double hydroxide nanoparticles and its cellular internalization for possible treatment of neurodegenerative diseases. J. Drug Deliv. Sci. Technol. 52, 500–508. https://doi.org/10.1016/j.jddst.2019.05.008

Balbuena, J., Cruz-Yusta, M., Sánchez, L., 2015. Nanomaterials to Combat NO_x Pollution. J. Nanosci. Nanotechnol. 15, 6373–6385. https://doi.org/10.1166/jnn.2015.10871

Cavani, F., Trifirò, F., Vaccari, A., 1991. Hydrotalcite-type anionic clays: Preparation, properties and applications. Catal. Today 11, 173–301. https://doi.org/https://doi.org/10.1016/0920-5861(91)80068-K

Chaara, D., Bruna, F., Draoui, K., Ulibarri, M.A., Barriga, C., Pavlovic, I., 2012. Applied Clay Science Study of key parameters affecting adsorption of the herbicide Linuron on organohydrotalcites. Appl. Clay Sci. 58, 34–38. https://doi.org/10.1016/j.clay.2012.01.008

Chao, H.-P., Wang, Y.-C., Tran, H.N., 2018. Removal of hexavalent chromium from groundwater by Mg/Al-layered double hydroxides using characteristics of in-situ synthesis. Environ. Pollut. 243, 620–629. https://doi.org/10.1016/j.envpol.2018.08.033

Chen, B.H., Hong, C.J., Kan, H.D., 2004. Exposures and health outcomes from outdoor air

pollutants in China. Toxicology 198, 291–300. https://doi.org/10.1016/j.tox.2004.02.005

Chen, P., Liu, H., Sun, Y., Li, J., Cui, W., Wang, L., Zhang, W., Yuan, X., Wang, Z., Zhang, Y., Dong, F., 2020. Bi metal prevents the deactivation of oxygen vacancies in $Bi_2O_2CO_3$ for stable and efficient photocatalytic NO abatement. Appl. Catal. B Environ. 264. https://doi.org/10.1016/j.apcatb.2019.118545

Comelli, N.A., Ruiz, M.L., Merino, N.A., Lick, I.D., Rodríguez-Castellón, E., Jiménez-López, A., Ponzi, M.I., 2013. Preparation and characterisation of calcined Mg/Al hydrotalcites impregnated with alkaline nitrate and their activities in the combustion of particulate matter. Appl. Clay Sci. 80–81, 426–432. https://doi.org/https://doi.org/10.1016/j.clay.2013.05.013

Costantino, U., Casciola, M., Massinelli, L., Nocchetti, M., Vivani, R., 1997. Intercalation and grafting of hydrogen phosphates and phosphonates into synthetic hydrotalcites and ac-conductivity of the compounds thereby obtained. Solid State Ionics 97, 203–212. https://doi.org/https://doi.org/10.1016/S0167-2738(97)00043-X

del Arco, M., Carriazo, D., Gutiérrez, S., Martín, C., Rives, V., 2004. Synthesis and Characterization of New Mg_2Al-Paratungstate Layered Double Hydroxides. Inorg. Chem. 43, 375–384. https://doi.org/10.1021/ic0347790

del Arco, M., Carriazo, D., Martín, C., Pérez Grueso, A.M., Rives, V., 2006. Characterization of chromate-intercalated layered double hydroxides, in: Materials Science Forum. Trans Tech Publ, pp. 1541–1545.

European Environment Agency, 2019. Air quality in Europe-2019 report. https://doi.org/10.2800/822355

Fei, Y., Liu, C., 2016. Chapter 12 - Detoxification and Resource Recovery of Chromium-Containing

427 Wastes, in: Prasad, M.N. V, Shih, K. (Eds.), Environmental Materials and Waste. Academic
428 Press, pp. 265–284. https://doi.org/https://doi.org/10.1016/B978-0-12-803837-6.00012-3
429 Fragoso, J., Oliva, M.A., Camacho, L., Cruz-Yusta, M., de Miguel, G., Martin, F., Pastor, A.,
430 Pavlovic, I., Sánchez, L., 2021. Insight into the role of copper in the promoted photocatalytic
431 removal of NO using $Zn_{2-x}Cu_xCr$-CO3 layered double hydroxide. Chemosphere 275, 130030.
432 https://doi.org/https://doi.org/10.1016/j.chemosphere.2021.130030
433 Frost, R.L., Musumeci, A.W., Bostrom, T., Adebajo, M.O., Weier, M.L., Martens, W., 2005.
434 Thermal decomposition of hydrotalcite with chromate, molybdate or sulphate in the
435 interlayer. Thermochim. Acta 429, 179–187.
436 https://doi.org/https://doi.org/10.1016/j.tca.2005.03.014
437 Gao, G., Zhu, Z., Zheng, J., Liu, Z., Wang, Q., Yan, Y., 2019. Ultrathin magnetic Mg-Al LDH
438 photocatalyst for enhanced CO_2 reduction: Fabrication and mechanism. J. Colloid Interface
439 Sci. 555, 1–10. https://doi.org/https://doi.org/10.1016/j.jcis.2019.07.025
440 Goh, K.-H., Lim, T.-T., Dong, Z., 2008. Application of layered double hydroxides for removal of
441 oxyanions: A review. Water Res. 42, 1343–1368.
442 https://doi.org/https://doi.org/10.1016/j.watres.2007.10.043
443 González, M.A., Trócoli, R., Pavlovic, I., Barriga, C., Mantia, F. La, 2016. Electrochemistry
444 Communications Layered double hydroxides as a suitable substrate to improve the
445 efficiency of Zn anode in neutral pH Zn-ion batteries. Electrochem. commun. 68, 1–4.
446 https://doi.org/10.1016/j.elecom.2016.04.006
447 Hsu, L., Tzou, Y., Chiang, P., Fu, W., Wang, M., Yi, H., Liu, Y., 2019. Adsorption mechanisms of
448 chromate and phosphate on hydrotalcite : A combination of macroscopic and spectroscopic
449 studies *. Environ. Pollut. 247, 180–187. https://doi.org/10.1016/j.envpol.2019.01.012

Huo, W., Cao, T., Liu, X., Xu, W., Dong, B., Zhang, Y., Dong, F., 2019a. Anion intercalated layered-double-hydroxide structure for efficient photocatalytic NO remove. Green energy&Environ. 4, 270–277. https://doi.org/10.1016/j.gee.2018.11.001

Huo, W., Xu, W., Cao, T., Liu, X., Zhang, Y., Dong, F., 2019b. Carbonate-intercalated defective bismuth tungstate for efficiently photocatalytic NO removal and promotion mechanism study. Appl. Catal. B Environ. 254, 206–213. https://doi.org/10.1016/j.apcatb.2019.04.099

Jin, L., Zeng, H.Y., Du, J.Z., Xu, S., 2020. Intercalation of organic and inorganic anions into layered double hydroxides for polymer flame retardancy. Appl. Clay Sci. 187, 105481. https://doi.org/10.1016/j.clay.2020.105481

Jobbágy, M., Regazzoni, A.E., 2013. Complexation at the edges of hydrotalcite: The cases of arsenate and chromate. J. Colloid Interface Sci. 393, 314–318. https://doi.org/https://doi.org/10.1016/j.jcis.2012.10.069

Kaprara, E., Kazakis, N., Simeonidis, K., Coles, S., Zouboulis, A.I., Samaras, P., Mitrakas, M., 2015. Occurrence of Cr(VI) in drinking water of Greece and relation to the geological background. J. Hazard. Mater. 281, 2–11. https://doi.org/10.1016/j.jhazmat.2014.06.084

Kim, H.-J., Lee, J.Y., Kim, T.-H., Gwak, G.-H., Park, J.H., Oh, J.-M., 2020. Radioisotope and anticancer agent incorporated layered double hydroxide for tumor targeting theranostic nanomedicine. Appl. Clay Sci. 186. https://doi.org/10.1016/j.clay.2020.105454

Koleli, N., Demir, A., 2016. Chapter 11 - Chromite, in: Prasad, M.N. V, Shih, K. (Eds.), Environmental Materials and Waste. Academic Press, pp. 245–263. https://doi.org/https://doi.org/10.1016/B978-0-12-803837-6.00011-1

Kuncewicz, J., Ząbek, P., Stochel, G., Stasicka, Z., Macyk, W., 2011. Visible light driven photocatalysis in chromate(VI)/TiO_2 systems—Improving stability of the photocatalyst.

Catal. Today 161, 78–83. https://doi.org/https://doi.org/10.1016/j.cattod.2010.10.075

Lazaridis, N.K., Pandi, T.A., Matis, K.A., 2004. Chromium(VI) Removal from Aqueous Solutions by Mg–Al–CO_3 Hydrotalcite: Sorption–Desorption Kinetic and Equilibrium Studies. Ind. Eng. Chem. Res. 43, 2209–2215. https://doi.org/10.1021/ie030735n

Lewis, R.J., 2012. Sax's Dangerous Properties of Industrial Materials, 5 Volume Set, 12th Edition, Twelth. ed. Wiley & Sons, New Jersey.

Li, X., Zhang, W., Cui, W., Li, J., Sun, Y., Jiang, G., Huang, H., Zhang, Y., Dong, F., 2019. Reactant activation and photocatalysis mechanisms on Bi-metal@Bi_2GeO_5 with oxygen vacancies: A combined experimental and theoretical investigation. Chem. Eng. J. 370, 1366–1375. https://doi.org/10.1016/j.cej.2019.04.003

Liao, J., Cui, W., Li, J., Sheng, J., Wang, H., Dong, X., Chen, P., Jiang, G., Wang, Z., Dong, F., 2020. Nitrogen defect structure and NO+ intermediate promoted photocatalytic NO removal on H_2 treated g-C_3N_4. Chem. Eng. J. 379. https://doi.org/10.1016/j.cej.2019.122282

Lu, Y., Jiang, B., Fang, L., Ling, F., Gao, J., Wu, F., Zhang, X., 2016. High performance NiFe layered double hydroxide for methyl orange dye and Cr(VI) adsorption. Chemosphere 152, 415–422. https://doi.org/10.1016/j.chemosphere.2016.03.015

Lv, X., Zhang, J., Dong, X., Pan, J., Zhang, W., Wang, W., Jiang, G., Dong, F., 2020. Layered double hydroxide nanosheets as efficient photocatalysts for NO removal: Band structure engineering and surface hydroxyl ions activation. Appl. Catal. B Environ. 277, 119200. https://doi.org/https://doi.org/10.1016/j.apcatb.2020.119200

Malherbe, F., Bigey, L., Forano, C., de Roy, A., Besse, J.-P., 1999. Structural aspects and thermal properties of takovite-like layered double hydroxides pillared with chromium oxo-anions. J. Chem. Soc. Dalt. Trans. 3831–3839. https://doi.org/10.1039/A903766G

Mantilla, A., Jácome-Acatitla, G., Morales-Mendoza, G., Tzompantzi, F., Gómez, R., 2011. Photoassisted Degradation of 4-Chlorophenol and p-Cresol Using MgAl Hydrotalcites. Ind. Eng. Chem. Res. 50, 2762–2767. https://doi.org/10.1021/ie1006883

Mantilla, A., Tzompantzi, F., Fernández, J.L., Díaz Góngora, J.A.I., Mendoza, G., Gómez, R., 2010. Photodegradation of 2,4-dichlorophenoxyacetic acid using ZnAlFe layered double hydroxides as photocatalysts. Catal. Today 148, 119–123. https://doi.org/10.1016/j.cattod.2009.02.036

Mohapatra, L., Parida, K., 2016. A review on the recent progress, challenges and perspective of layered double hydroxides as promising photocatalysts. J. Mater. Chem. A 4, 10744–10766. https://doi.org/10.1039/C6TA01668E

Mohapatra, L., Parida, K., Satpathy, M., 2012. Molybdate/Tungstate Intercalated Oxo-Bridged Zn/Y LDH for Solar Light Induced Photodegradation of Organic Pollutants. J. Phys. Chem. C 116, 13063–13070. https://doi.org/10.1021/jp300066g

Olszówka, J.E., Karcz, R., Napruszewska, B.D., Michalik-Zym, A., Duraczyńska, D., Kryściak-Czerwenka, J., Niecikowska, A., Bahranowski, K., Serwicka, E.M., 2018. Effect of MgAl hydrotalcite crystallinity on catalytic Baeyer-Villiger oxidation of cyclohexanone with H_2O_2/acetonitrile. Catal. Commun. 107, 48–52. https://doi.org/https://doi.org/10.1016/j.catcom.2018.01.014

Otero, R., Fernández, J.M., González, M.A., Pavlovic, I., Ulibarri, M.A., 2013. Pesticides adsorption – desorption on Mg – Al mixed oxides . Kinetic modeling , competing factors and recyclability. Chem. Eng. J. 221, 214–221. https://doi.org/10.1016/j.cej.2013.02.007

Paikaray, S., Hendry, M.J., Essil, J., 2013. Controls on arsenate , molybdate , and selenate uptake by hydrotalcite-like layered double hydroxides 345, 130–138.

519 https://doi.org/10.1016/j.chemgeo.2013.02.015
520 Parida, K., Mohapatra, L., 2012. Recent progress in the development of carbonate-intercalated
521 Zn/Cr LDH as a novel photocatalyst for hydrogen evolution aimed at the utilization of solar
522 light. Dalt. Trans. 41, 1173–1178. https://doi.org/10.1039/C1DT10957J
523 Parida, K., Satpathy, M., Mohapatra, L., 2012. Incorporation of Fe^{3+} into Mg/Al layered double
524 hydroxide framework: Effects on textural properties and photocatalytic activity for H_2
525 generation. J. Mater. Chem. 22, 7350–7357. https://doi.org/10.1039/c2jm15658j
526 Pastor, A., Rodriguez-Rivas, F., de Miguel, G., Cruz-Yusta, M., Martin, F., Pavlovic, I., Sanchez, L.,
527 2020. Effects of Fe^{3+} substitution on Zn-Al layered double hydroxides for enhanced NO
528 photochemical abatement. Chem. Eng. J. 387. https://doi.org/10.1016/j.cej.2020.124110
529 Pavlovic, I., González, M.A., Ulibarri, M.A., Barriga, C., 2013. Applied Clay Science Caprylate
530 intercalated layered double hydroxide as adsorbent of the linuron , 2, 4-DB and metamitron
531 pesticides from aqueous solution. Appl. Clay Sci. 80–81, 76–84.
532 https://doi.org/10.1016/j.clay.2013.06.008
533 Prasanna, S. V, Rao, R.A.P., Kamath, P.V., 2006. Layered double hydroxides as potential chromate
534 scavengers 304, 292–299. https://doi.org/10.1016/j.jcis.2006.08.064
535 Rives, V., 2001. Layered double hydroxides: present and future. Nova Publishers.
536 Rodriguez-Rivas, F., Pastor, A., Barriga, C., Cruz-Yusta, M., Sanchez, L., Pavlovic, I., 2018. Zn-Al
537 layered double hydroxides as efficient photocatalysts for NO_x abatement. Chem. Eng. J. 346,
538 151–158. https://doi.org/10.1016/j.cej.2018.04.022
539 Rodriguez-Rivas, F., Pastor, A., de Miguel, G., Cruz-Yusta, M., Pavlovic, I., Sanchez, L., 2020. Cr^{3+}
540 substituted Zn-Al layered double hydroxides as UV-Vis light photocatalysts for NO gas
541 removal from the urban environment. Sci. Total Environ. 706.

https://doi.org/10.1016/j.scitotenv.2019.136009

Taviot-Guého, C., Prévot, V., Forano, C., Renaudin, G., Mousty, C., Leroux, F., 2018. Tailoring Hybrid Layered Double Hydroxides for the Development of Innovative Applications. Adv. Funct. Mater. 28, 1–33. https://doi.org/10.1002/adfm.201703868

Tran, H.N., Nguyen, D.T., Le, G.T., Tomul, F., Lima, E.C., Woo, S.H., Sarmah, A.K., Nguyen, H.Q., Nguyen, P.T., Nguyen, D.D., Nguyen, T.V., Vigneswaran, S., Vo, D.-V.N., Chao, H.-P., 2019. Adsorption mechanism of hexavalent chromium onto layered double hydroxides-based adsorbents: A systematic in-depth review. J. Hazard. Mater. 373, 258–270. https://doi.org/10.1016/j.jhazmat.2019.03.018

Ukhurebor, K.E., Aigbe, U.O., Onyancha, R.B., Nwankwo, W., Osibote, O.A., Paumo, H.K., Ama, O.M., Adetunji, C.O., Siloko, I.U., 2021. Effect of hexavalent chromium on the environment and removal techniques: A review. J. Environ. Manage. 280, 111809. https://doi.org/10.1016/j.jenvman.2020.111809

Wu, M.J., Wu, J.Z., Zhang, J., Chen, H., Zhou, J.Z., Qian, G.R., Xu, Z.P., Du, Z., Rao, Q.L., 2018. A review on fabricating heterostructures from layered double hydroxides for enhanced photocatalytic activities. Catal. Sci. Technol. 8, 1207–1228. https://doi.org/10.1039/C7CY02314F

Zhang, W., Dong, X., Liang, Y., Sun, Y., Dong, F., 2018. Ag/AgCl nanoparticles assembled on BiOCl/$Bi_{12}O_{17}Cl_2$ nanosheets: Enhanced plasmonic visible light photocatalysis and in situ DRIFTS investigation. Appl. Surf. Sci. 455, 236–243. https://doi.org/10.1016/j.apsusc.2018.05.171

Zheng, T.-R., Qian, L.-L., Li, M., Wang, Z.-X., Li, K., Zhang, Y.-Q., Li, B.-L., Wu, B., 2018. A bifunctional cationic metal–organic framework based on unprecedented nonanuclear

565 copper(ii) cluster for high dichromate and chromate trapping and highly efficient
566 photocatalytic degradation of organic dyes under visible light irradiation. Dalt. Trans. 47,
567 9103–9113. https://doi.org/10.1039/C8DT01685B
568 Zhou, W., Zhai, S., Pan, J., Cui, A., Qian, J., He, M., Xu, Z., Chen, Q., 2017. Bifunctional NiGa
569 Layered Double Hydroxide for the Aerobic Oxidation/Condensation Tandem Reaction
570 between Aromatic Alcohols and Active Methylene Compounds. Asian J. Org. Chem. 6,
571 1536–1541. https://doi.org/10.1002/ajoc.201700352
572